Jurnal Ilmu Fisika
Vol. 17, No. 1, March 2025, pp. 63–77
ISSN: 1979-4657 (Print); 2614-7386 (Online)
https://doi.org/10.25077/jif.17.1.63-77.2025

Freeze-Thawed PVA Hydrogel Loaded by *Morinda Citrifolia* L. Leaves Extract with Physical and In-Vitro Antibacterial Properties

Kusjuriansah Kusjuriansah[1], Ade Mufti[1], Fauzah Nilva Tulhana[1], Dinny Fauziah[2]

[1] Department of Physics, Universitas Halim Sanusi, Bandung, 40262, Indonesia.
[2] Department of Agrotechnology, Universitas Halim Sanusi, Bandung, 40262, Indonesia.

Article Info

Article History:

Received January 14, 2025
Revised February 26, 2025
Accepted March 02, 2025
Published March 04, 2025

Keywords:

polyvinyl alcohol
hydrogel
Morinda citrifolia L. leaves extract
freeze-thaw
antibacterial

Corresponding Author:

Kusjuriansah Kusjuriansah,
Email: kusjuriansah714@gmail.com

ABSTRACT

Morinda citrifolia L. leaves extract (MCLE) has been used as a medical material because of its antibacterial properties. Hydrogels synthesized from polyvinyl alcohol (PVA) are known to be applicable as delivery media for antibacterial substances. This article reports using the freeze-thaw method to use PVA hydrogel as an encapsulation medium for MCLE. PVA/MCLE hydrogel was synthesized in several combinations, namely 10:0, 10:1, 10:2, 10:3, 10:4, and 10:5. The test results showed the conductivity and pH values of the precursor solution increased as the extract fraction increased, but decreased in the viscosity. The hydrogel showed a morphology with increased pore size when the extract fraction in the hydrogel increased. FTIR characterization confirmed that the extract had been successfully loaded into the hydrogel. The swelling degree test of the hydrogels showed an increase for samples 10:1 to 10:3 and a decrease for samples 10:4 to 10:5. Increasing the extract fraction then resulted in a decrease in the gel fraction of the hydrogel. The antibacterial activity test confirmed that the antibacterial activity in the extract remained present after being encapsulated in the hydrogel. Thus, the addition of MCLE affects the performance of the hydrogels to be applied in the medical field.

1. INTRODUCTION

Hydrogel is a material composed of a three-dimensional polymer network that has the ability to absorb liquids. Hydrogels have properties similar to natural living tissue, with high water content and porosity (Caló & Khutoryanskiy, 2015). Natural, synthetic, and mixed polymers have been widely used to synthesize hydrogel. Hydrogels from natural polymers have excellent biocompatibility properties but poor mechanical properties (Zhao et al., 2023), such as chitosan (Hong et al., 2024) and alginate (Savić Gajić et al., 2023). On the other hand, synthetic polymers such as polyvinyl alcohol (PVA) (Liang et al., 2024) and poly (ethylene glycol) (PEG) (Wang et al., 2023) have also been used to make hydrogels because they have physical and chemical properties that can be adjusted according to needs (Bashir et al., 2020). PVA is a synthetic polymer easily soluble in water and has hydroxyl functional groups that can be cross-linked to form hydrogels with high mechanical strength (Chen et al., 2022). There are two methods for synthesizing hydrogels, namely chemical and physical cross-linking. Chemical cross-linking methods can produce hydrogels with excellent mechanical properties, such as cross-linking with

aldehydes (Parhi, 2017) and enzymes (Naranjo-alcazar et al., 2023). However, the cross-linking agent must be extracted from the hydrogel before application because it carries toxic properties (Akhtar et al., 2016). Hydrogel synthesis methods that are safe from toxic properties can be carried out through physical cross-linking, one of which is freeze-thaw (Edikresnha et al., 2021). Freeze-thaw is carried out in several freezing and thawing cycles to form a hydrogel through a crystallization process to control its physical and chemical properties (Bustamante-Torres et al., 2021). Hydrogels synthesized from PVA polymer using the freeze-thaw method are known to be widely developed for medical applications (Waresindo et al., 2021; Luthfianti et al., 2022).

On the other hand, Indonesia is a tropical country known to have a variety of natural ingredients that can be used in the medical field. *Morinda citrifolia* L. is one of the natural ingredients that has been widely used for traditional medicines since ancient times, as a dressing for injured skin (Sabirin et al., 2013), a cream to speed up wound healing (Parmadi et al., 2019), and an antibacterial agent (Erina et al., 2019). Through phytochemical analysis, *Morinda citrifolia* L. leaves contain several chemical compounds, such as saponins, tannins, triterpenoids, alkaloids, and flavonoids. (Nayak et al., 2009). Flavonoids, tannins, and saponins have been reported to have high antibacterial activity (Halimah et al., 2019; Claudya et al., 2023). A suitable delivery medium is required for the antibacterial activity in Morinda citrifolia L. leaves. Presenting suitable and easy-to-use delivery media is a challenge that needs to be overcome. In the last few years, hydrogel has been widely developed as a material that can be used as a delivery medium for antibacterial agents (Edikresnha et al., 2021; Waresindo et al., 2021; Luthfianti et al., 2022). Hydrogels are known to own several advantages, such as being easy to use, easy to clean, and having intermolecular forces that can reduce molecular mobility so that they can encapsulate drugs stably (Saputro et al., 2021). This research will use PVA hydrogel as a delivery medium to encapsulate *Morinda citrifolia* L. leaves extract (MCLE).

Although much research has been carried out on MCLE, there has not been much research using hydrogel as a matrix to encapsulate MCLE. Therefore, this study aims to develop and characterize a composite hydrogel from PVA and MCLE, which was synthesized using the freeze-thaw method. The main novelty in this research is that the PVA hydrogel initially did not have antibacterial properties. However, after MCLE loading, the composite hydrogel could have antibacterial activity. The synthesized hydrogel was then characterized physically and pharmacologically. The physical characterization carried out includes testing the physical properties of the precursor solution (conductivity, viscosity, and pH), Scanning Electron Microscope (SEM), Fourier Transform Infrared (FTIR), swelling degree, and gel fraction. The pharmacological characterization carried out was an in-vitro antibacterial activity test.

2. METHOD

2.1 Materials

PVA fully hydrolyzed was obtained from Sigma-Aldrich. Analytical ethanol was obtained from Merck, Germany. Aquades were obtained from ROFA Laboratory Center, Bandung. *Morinda citrifolia* L. leaves were obtained from Bantul Regency, Yogyakarta, Indonesia.

2.2 Preparation of MCLE

Morinda citrifolia L. leaves are extracted using the maceration method. The *Morinda citrifolia* L. leaves that have been collected are first dried and ground into powder. Powder of *Morinda citrifolia* L. leaves are then filtered in a size of mesh-60. The *Morinda citrifolia* L. leaves powder is soaked in 96% (v/v) ethanol solvent. The mass ratio of *Morinda citrifolia* L. leaves to powder and ethanol is 1:10. The soaking process lasts 1 x 24 hours, accompanied by regular stirring. After that, the filtering process is carried out using flannel cloth to obtain the filtrate. The soaking and filtering process is repeated with half the previous ethanol ratio (1:5). The filtrate is then collected and evaporated using a rotary evaporator to obtain a thick MCLE (Mohammad & Yulyianti, 2023).

2.3 Preparation of the precursor solutions and the hydrogels

In this study, the initial solutions prepared were PVA and MCLE solutions. The PVA solution was prepared with a concentration of 10% (w/w) by dissolving the PVA powder in distilled water, then stirring using a magnetic stirrer at 100ºC for 2 hours until mixed well. In addition, the MCLE solution was prepared with a concentration of 10% (w/w) by dissolving the MCLE in a mixture of solvents (aquades and ethanol with a 1:1 ratio), then stirring using a magnetic stirrer until evenly mixed. After that, the PVA and MCLE solutions were mixed in various weight ratios, namely 10:0, 10:1, 10:2, 10:3, 10:4, and 10:5, then stirred using a magnetic stirrer until evenly mixed. The solution is then put in a potzalp to be synthesized into hydrogel via the freeze-thaw method. The freezing process lasted 20 hours at -25oC, while the thawing process was carried out for 4 hours at room temperature. The freeze-thaw process is repeated for six cycles (Edikresnha et al., 2021). A total of six freeze-thaw cycles were selected after observing the hydrogel formation in each freeze-thaw cycle. After one to five freeze-thaw cycles, the hydrogel formed was still soft or had poor mechanical properties. In six freeze-thaw cycles, a hydrogel was formed with good mechanical properties. Meanwhile, if the freeze-thaw cycle exceeds six, the hydrogel will be produced with mechanical properties that are too hard. The successfully synthesized hydrogel is shown in Figure 1.

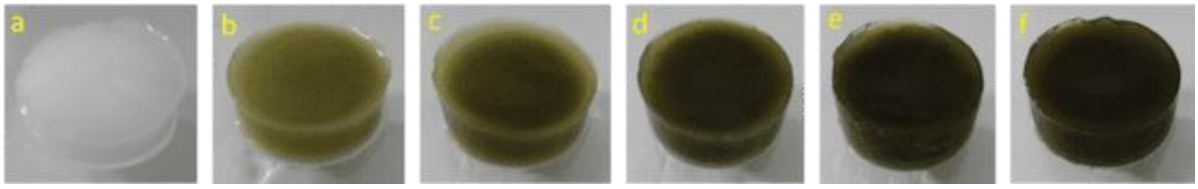

Figure 1. Results of hydrogel synthesis for sample (a) 10:0, (b) 10:1, (c) 10:2, (d) 10:3, (e) 10:4, dan (f) 10:5.

2.4 The characterizations of precursor solutions

The precursor solution is previously analyzed to determine viscosity, conductivity, and pH properties. The viscosity of the solution was determined using a Fisher Scientific Ostwald-Fenske viscometer, Surface Tensiomat model 21. Meanwhile, the conductivity of the solution was measured using a conductometer. The pH value of the solution is measured with a pH meter brand Orion.

2.5 *Scanning Electron Microscope* (SEM)

SEM characterization was carried out to examine the internal morphology of the synthesized hydrogel. Before the SEM characterization, the hydrogel was dried using the freeze-dry method. The dried hydrogel is then cut in a plane parallel to the cylinder axis. Afterward, the hydrogel surface was scanned using SEM. In this research, hydrogel morphology observations were carried out using an SEM device with an excitation voltage of 10 kV in the Chemistry Laboratory of FMIPA ITB. Hydrogel morphology observations were carried out at 1,000 and 5,000 times magnification.

2.6 *Fourier-Transform Infrared Spectroscopy* (FTIR)

FTIR characterization was carried out to see the functional groups of the hydrogel that were affected by the presence of MCLE. In this study, the determination of functional groups in hydrogels was carried out using a Fourier-Transform Infrared Spectroscopy (FTIR) tool (Bruker, Alpha Platinum ATR A220/D-01) available at the Chemistry Laboratory of FMIPA ITB. Determination of functional groups in hydrogels using the FTIR tool is carried out in the wave number range between 500 to 4500 cm^{-1}.

2.7 The swelling degree of the hydrogels

The swelling degree test was carried out to determine the ability of the hydrogel to absorb liquid. Before testing, the hydrogel was dried at 50ºC in the oven until the mass remained constant. The dried hydrogel was then soaked in a container filled with phosphate buffer saline (PBS) with a pH of 7.4 and stored at room temperature. Hydrogel mass measurements were performed at 0, 3, 6, 9, 12, 24, and 48 hours. Before these measurements, the surface of the hydrogel was dried first using filter paper. The ratio between the increase in the mass of the hydrogel after soaking and the mass of the hydrogel before

soaking is defined as the swelling degree. The swelling degree is expressed by the following formula (1) (Waresindo et al., 2021).

$$\text{Swelling degree (\%)} = \frac{w_2 - w_1}{w_1} \times 100\% \quad (1)$$

with w_2 shows the mass of the hydrogel after soaking for the specified time and w_1 Shows the mass of the hydrogel before soaking.

2.8 The gel fractions

After testing the swelling degree, the drying process of the hydrogel was carried out again in the oven at 50ºC until the mass remained constant. The mass of the hydrogel obtained after the drying process is expressed as w_3. The gel fraction is then defined as the ratio between the masses of the hydrogel after drying again (w_3) and the mass of the hydrogel before immersion (w_1), as stated in equation (2) below (Edikresnha et al., 2021).

$$\text{Gel fraction (\%)} = \frac{w_3}{w_1} \times 100\% \quad (2)$$

2.9 Antibacterial activity

The method used to test the antibacterial activity of hydrogels is the agar diffusion method (Luthfianti et al., 2022). We use gram-positive bacteria viz Staphylococcus aureus (ATCC 6538) and gram-negative bacteria viz *Pseudomonas aeruginosa* (ATCC 9027) to validate antibacterial effectiveness. Then, a hydrogel with a thickness of about 5 mm and a diameter of about 24 mm was prepared for testing. The mass of the hydrogel was then weighed and sterilized with UV light. *Muller Hinton Agar* (MHA) media as bottom agar was prepared in a petri dish. Hydrogel was then placed on top of the MHA media. The hydrogel is then administered top agar, *which contains MHA media and bacteria tests evenly over the entire surface of the* bottom order. The same procedure was carried out for bacterial control without hydrogel for both positive and harmful bacteria. The incubation process was then carried out at 37ºC within 24 hours. After that, the bacterial inhibition zone was measured using a caliper. From the inhibition zone, 50 µL top agar was taken to undergo the dilution process in NaCl solution. A total of 500 μL from the dilution results is then taken and placed on top of the MHA media until evenly distributed over the surface. After that, the incubation process was repeated at 37ºC in 24 hours. The number of bacterial colonies that grow is then counted to determine the antibacterial activity of the hydrogel. The antibacterial activity is calculated using Equation (3) below (Waresindo et al., 2021).

$$\text{Antibacterial activity} = \frac{\left[\left(\log \text{control (cfu.ml}^{-1}\text{)}\right) - \left(\log \text{hydrogel (cfu.ml}^{-1}\text{)}\right)\right]}{\text{mass (gram)}.\left(\log \text{control (cfu.ml}^{-1}\text{)}\right)} \quad (3)$$

3. RESULTS AND DISCUSSION

3.1 Properties of precursor solutions

The results of measuring the conductivity, viscosity, and pH of the precursor solution are presented in Table 1. The conductivity value shows a measure of the ability of a solution to conduct electricity. The greater the solute in a solution, the greater the number of ions and the greater the conductivity (Irwan et al., 2016). The MCLE solution showed higher conductivity values than the 10:0 solution. Therefore, the loading of the MCLE solution then increases the conductivity values. As the MCLE solution fraction increases, the conductivity value of the mixed solution from samples 10:1 to 10:5 also increases. The conductivity values of the precursor solutions are in the range of 12.8733 to 16.6100 µS/cm. This conductivity value influences the performance of the hydrogel in increasing endogenous electrical current in the skin, which will encourage neutrophils, macrophages, and keratinocytes to the wound site, thereby accelerating wound healing (Qiao et al., 2023). The measure of the thickness of a solution is then expressed as viscosity (Stabik et al., 2009). The 10:0 solution has a greater viscosity than the MCLE solution, which shows that more of the constituent chains are bonded, so the viscosity is greater (Edikresnha et al., 2021). In the mixed solution, a decrease in viscosity was observed when the MCLE solution fraction was added. This is because the MCLE solution has a lower viscosity than the 10:0 solution, so the 10:1 to 10:5 samples experience a decrease in viscosity. The

viscosity value of the precursor solution influences the morphological structure of the resulting hydrogel, where the smaller the solution viscosity value produces the morphological structure of the hydrogel with larger pore sizes, as shown in the SEM image. For the hydrogel to be applied as a wound dressing, it is important to know the pH value of the precursor solution. Bacteria grow at a pH value of more than 6.0, so the pH value used is 4.0 to 6.0, according to the skin of humans (Edikresnha et al., 2019). In this study, the MCLE solution had a higher pH value than the 10:0 solution, so adding the MCLE solution fraction from the 10:1 to 10:5 sample increased the pH value. The pH value obtained from the 10:1 to 10:5 sample was 5.0133 to 5.8000, making it suitable for developing hydrogel as a wound dressing.

Table 1 Conductivity, viscosity, and pH of the precursor solution.

Sample Name	Conductivity (µS/cm)	Viscosity (cP)	pH
MCLE	559.3333 ± 0.5774	1.9333 ± 0.0035	6.2000 ± 0.0000
10:0	12.8733 ± 0.0115	121.8750 ± 0.0095	5.0133 ± 0.0058
10:1	13.4233 ± 0.0058	92.7917 ± 0.0135	5.5033 ± 0.0058
10:2	13.9533 ± 0.0058	67.4530 ± 0.0050	5.5367 ± 0.0058
10:3	14.6267 ± 0.0058	61.3030 ± 0.0095	5.5733 ± 0.0058
10:4	15.0633 ± 0.0115	47.3630 ± 0.0046	5.6533 ± 0.0115
10:5	16.6100 ± 0.0100	43.6920 ± 0.0090	5.8000 ± 0.0100

3.2 Scanning Electron Microscope (SEM)

The SEM observation results are presented in Figure 2 a). The 10:0 sample shows a non-porous surface. These results indicate that no solid and liquid phase separation was observed in the hydrogel composed of pure PVA. This is possible because the hydrogel collapses after undergoing the freeze-dry process (Edikresnha et al., 2021). On the other hand, 10:1 to 10:5 samples appear to show a porous surface. The size of the pores appears to be more significant as the extract fraction increases. This may be influenced by the composition of the extract solution in the hydrogel, where the extract is dissolved in ethanol/distilled water solvent in a ratio of 1:1. Ethanol is known to have a freezing point of around -114.1^{o}C (Anggraini et al., 2017)The hydrogel containing ethanol cannot completely dry during the freeze-dry process. This prevents the collapse process in the hydrogel so that the phase separation can be observed in the presence of a porous surface. Phase separation is the process of separating frozen liquid and forming PVA crystals during the freeze-thaw process. This causes the emergence of areas that are rich in PVA (solid areas) and areas that are rare in PVA (liquid areas), which will become pores after freeze-dry (Bercea, 2024). From 10:1 to 10:5 samples, the pore size appears larger due to the increasing number of ethanol fractions in the hydrogel that cannot be dried through freeze-dry and the smaller PVA fraction as the main component. The pore size of the composite hydrogel was determined using ImageJ software (Waresindo et al., 2021). The pore size distribution of the composite hydrogel was obtained through non-linear curve fitting in OriginPro 8.5.1 software with a Gaussian peak function. Composite hydrogel samples from 10:1 to 10:5, respectively, showed a pore size distribution of approximately 2.58 ± 0.19, 3.54 ± 0.13, 6.97 ± 0.25, 7.75 ± 1.54 and 8.23 ± 0.89 µm. Hydrogel with high porosity supports the absorption of wound fluid and the distribution of oxygel to injured skin (Maeso et al., 2024). The phase separation in the composite hydrogel has been observed through SEM images.

3.3 Fourier-Transform Infrared Spectroscopy (FTIR)

The FTIR spectrum results of the PVA, MCLE, and hydrogel samples are shown in Figure 3. The PVA powder is known to have several peaks, namely at 3425, 2939, 1635, 1444, 1328, 1143, and 1097 cm^{-1}. The peak at 3425 cm^{-1} shows O-H stretching vibrations, while CH_2 asymmetric stretching vibrations are indicated by a peak around 2939 cm^{1} (Zidan et al., 2019). The peak is around 1635 cm^{-1}, related to C=O stretching vibrations, while the peak is around 1444 cm-1, representing the CH_2 bending vibrations (Ramadhani et al., 2021). The peak at 1328 cm^{-1} refers to the C-H bending vibration (T et al.,

2023), while the peak at 1143 cm^{-1} describes C-O-C stretching vibrations (Hooi et al., 2021). Also, the peak at 1097 cm^{-1} demonstrated the C–O–C stretching vibrations characteristic of the main chain of PVA (Lazidou et al., 2019).

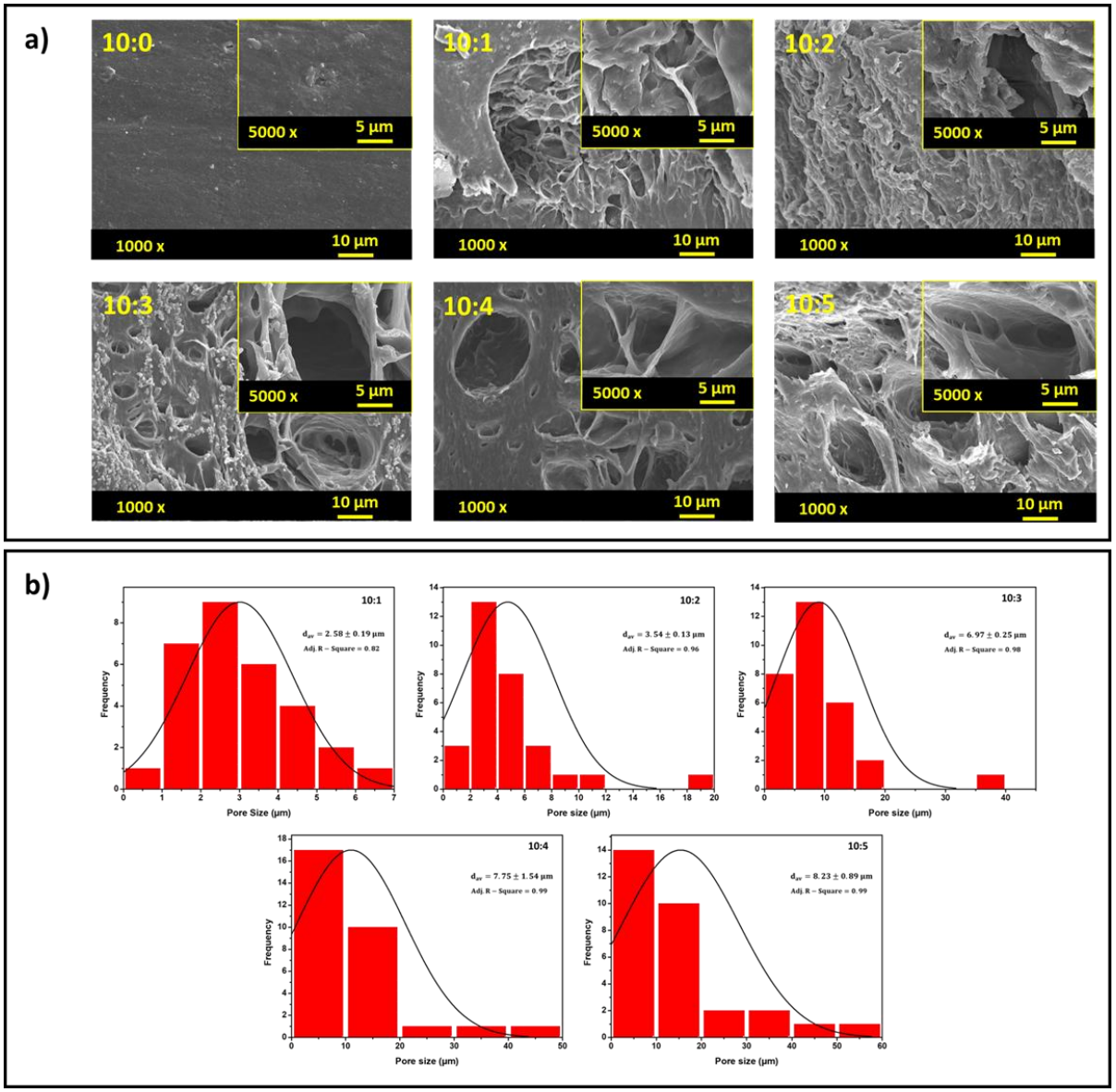

Figure 2 a) SEM image for composite hydrogels, **b)** pore size distributions of composite hydrogels based on non-linear curve fitting on OriginPro 8.5.1 software with the Gaussian as the peak function.

On the other hand, the MCLE sample shows several peaks, namely at 3410, 2924, 2852, 1631, 1384, and 1058 cm^{-1}. The peak is about 3410 cm^{-1} related to the O–H group with the type of phenolic compound. Phenolic compounds are antibacterial agents that interfere with the cytoplasmic membrane's function by preventing energy formation and inhibiting bacterial motility (Pertiwi et al., 2019), as confirmed by the results of antibacterial activity testing. Peaks at 2924 and 2852 cm^{-1} show the C-H functional group with the type of alkane compound (Sarkar et al., 2022). The peak is about 1631 cm^{-1} related to the C=C functional group with the type of alkene compound (Pertiwi et al., 2019). The peak at 1384 cm^{-1} is a C-H functional group with an alkane-type compound, while the C-O stretching vibration is represented by a peak around 1058 cm^{-1} (Pertiwi et al., 2019) (Sarkar et al., 2022). The characteristic peak for PVA (1097 cm^{-1}) is represented by a peak at 1095 cm^{-1} for hydrogels 10:0, 10:1, 10:4, and 10:5, while for hydrogels 10:2 and 10:3 are represented by peaks at 1093 and 1097 cm^{-1}, respectively.

The characteristic peak of PVA in all composite hydrogels indicates that all hydrogels have semicrystalline properties of PVA, which can maintain hydrogel stability (Hong et al., 2014). MCLE characteristic peak (3410 cm^{-1}) was observed for all composite hydrogels at slightly higher wavenumbers. These characteristic peaks are shown by wave numbers 3415, 3419, 3415, 3414, and 3415 for the 10:1, 10:2, 10:3, 10:4, and 10:5 composite hydrogels. The presence of the characteristic peak of MCLE then confirms that all composite hydrogels carry the antibacterial ability of MCLE. Thus, it can be concluded that PVA and MCLE have been contained in the composite hydrogel. The shifting characteristic peaks are possible due to chemical interactions between polymers after mixing, indicating a good miscibility level (Kamoun et al., 2015).

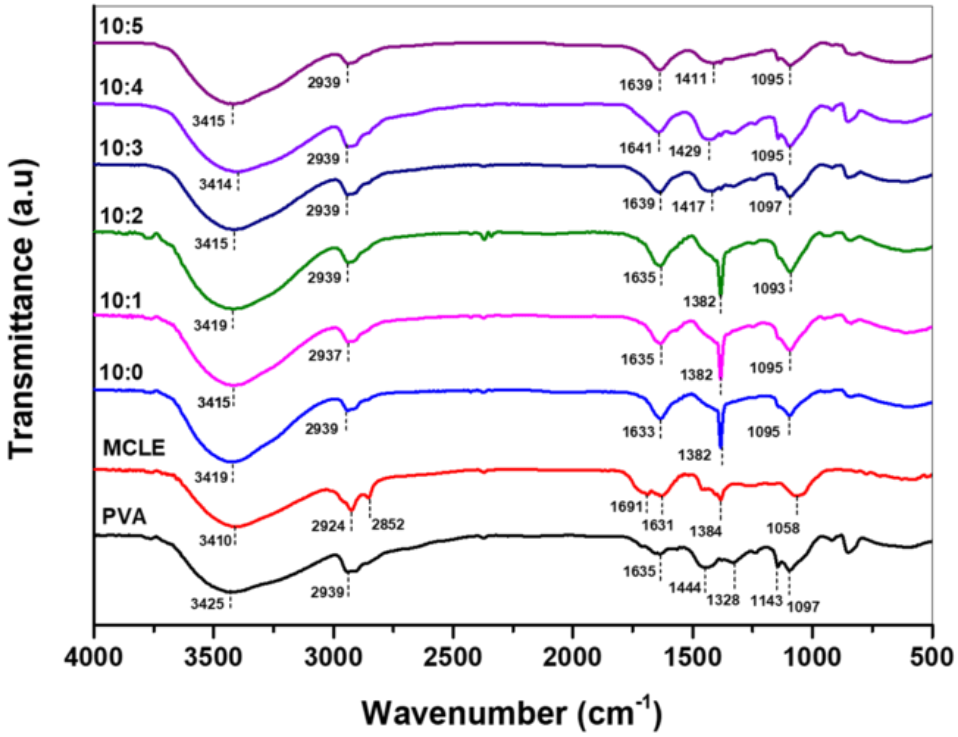

Figure 3 FTIR spectrum of PVA, MCLE, and hydrogel samples.

3.4 Swelling degree

The hydrogel samples showed their swelling degrees, as presented in Figure 4. Initially, all hydrogel samples showed a swelling degree that increased significantly in the first 6 hours. This initial swelling stage is related to the entry of PBS through the pores of the hydrogel surface, making the hydrogel network more flexible. It allows it to expand quickly through capillary effects (Zhang et al., 2022). That swelling degree then increased slowly in the 6th to 24th hours of testing. Moreover, we can see that the swelling degree tends to remain constant from the 24th to 48th hours. That final stage is related to swelling equilibrium, where the osmotic pressure and elastic contraction force in the hydrogel have reached a state dynamic balance (Wang et al., 2024). For the 48th hour, samples 10:0 to 10:5 have swelling degrees of about 125.18%, 135.47%, 142.86%, 181.51%, 169.19%, and 146.82%, respectively. These results indicate that the swelling degree tends to increase with increasing extract fraction for samples 10:0 to 10:3, then decreases for samples 10:4 to 10:5. The increase in the swelling degree for samples 10:0 to 10:3 is possible due to the effect of extract loading, which increases the pore size of the hydrogel thereby increasing the swelling degree of the hydrogel, as confirmed through SEM images (Waresindo et al., 2021). In addition, MCLE loading possibly decreased the cross-linking density in the composite hydrogel, as confirmed through the gel fraction results, thereby increasing the pores' size and water absorption ability. On the other hand, a decrease in the swelling degree for the 10:4 and 10:5 samples is possible due to the release of the extract during the testing process. The release of the extract occurs simultaneously with the absorption of PBS into the hydrogel so that the increase in hydrogel

weight due to PBS absorption will be reduced by the decrease in weight due to the release of the extract (Edikresnha et al., 2021). The release of the extract may occur more dominantly than the absorption of PBS into the hydrogel, thereby reducing the swelling degree of the composite hydrogels, as indicated by the change in the color of the PBS after testing, which became cloudy.

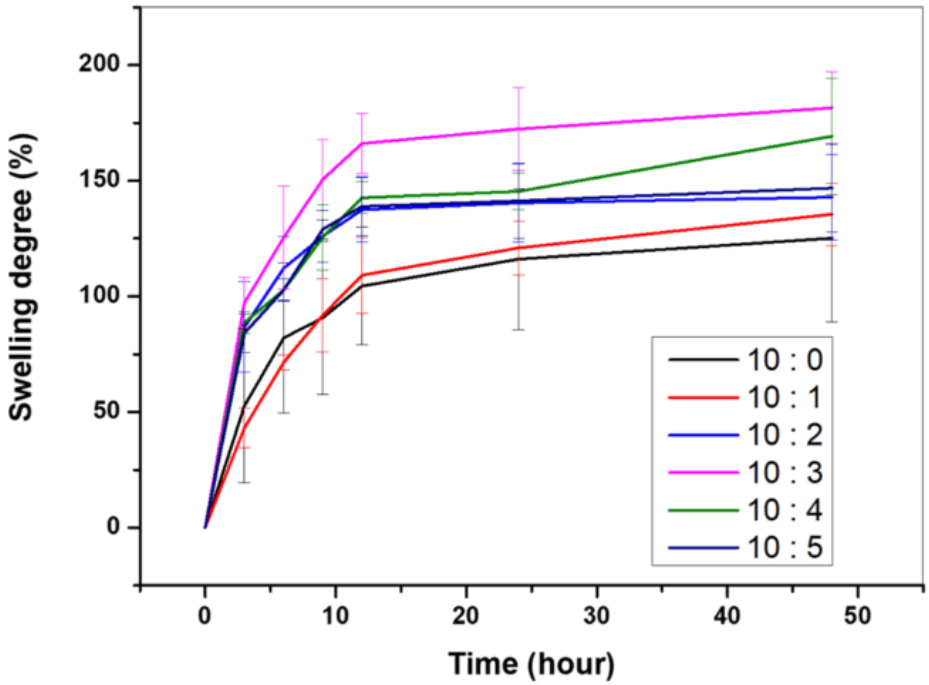

Figure 4 Swelling degree of hydrogel samples.

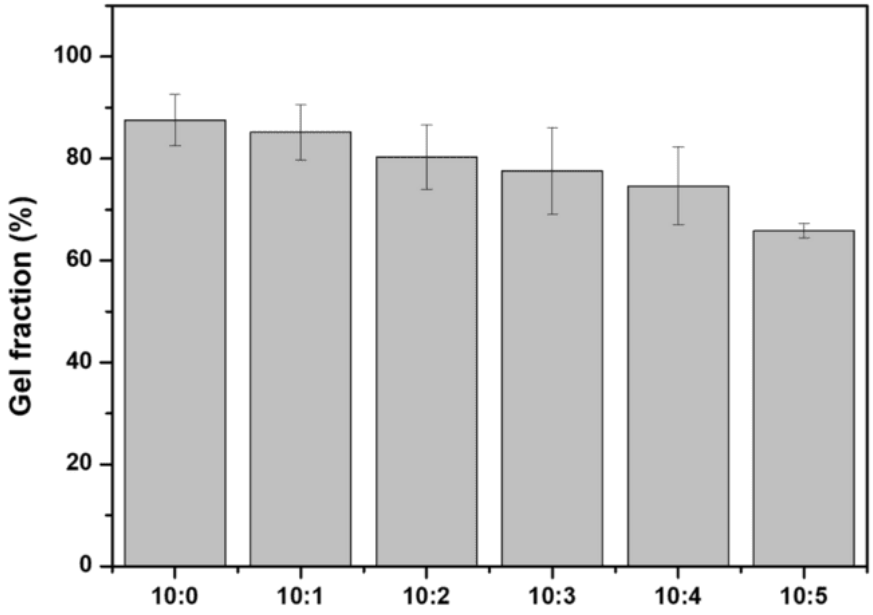

Figure 5 Gel fraction.

3.5 Gel fraction

Gel fraction testing was carried out to compare the masses of hydrogel after and before the swelling degree testing (Puspitasari et al., 2012). Before swelling degree testing, the PBS solution had a clear color. However, after swelling degree testing, the color of the PBS solution changed to cloudy, indicating the release of the extract from the hydrogel. This influences the change in hydrogel mass after testing, which was observed in the gel fraction value. The gel fraction also shows the effectiveness of

cross-links formation in the hydrogel, where the higher the gel fraction, the more cross-links are formed in the hydrogel (Halligan et al., 2023). The gel fraction values of each hydrogel sample are presented in Figure 5. Samples 10:0 to 10:5 showed gel fractions of 87.58 ± 5.01%, 85.18 ± 5.48%, 80.29 ± 6.33%, 77.65 ± 8.53%, 74.66 ± 7.59%, and 65.87 ± 1.38%, respectively. The 10:0 sample containing pure PVA has the largest gel fraction value, indicating the number of cross-links or monomer ions formed from the PVA group (Jayanudin et al., 2024). On the other hand, samples 10:1 to 10:5 decreased the gel fraction value as the extract fraction increased. This decrease indicates that the loading of the extract reduces the number of cross-links formed in the hydrogel (Maulidina et al., 2022). This is possible because the more the extract fraction in the hydrogel increases, the more extract release occurs during testing, resulting in a greater decrease in the hydrogel mass, which causes the gel fraction value to become smaller (Edikresnha et al., 2021).

3.6 Antibacterial activity

The antibacterial activity of all hydrogel samples was determined through two test methods, namely the disk diffusion method and the total plate number method. After 24 hours of incubation, the inhibition zone can be observed through the zone without bacterial growth around the hydrogel sample, as shown in Figure 6 and Figure 7. The diameter of the inhibition zone was then measured using a caliper for each hydrogel sample, and the results are presented in Table 2. The 10:0 sample did not produce an inhibitory zone diameter because PVA does not have antibacterial properties, so it cannot inhibit bacterial growth (Preda et al., 2023). On the other hand, samples 10:0 to 10:5 show a larger diameter of the inhibition zone. This is related to the antibacterial properties of MCLE (Erina et al., 2019), where adding the extract fraction to the hydrogel produces a more significant inhibition zone. MCLE is known to contain flavonoids, which can interact with bacterial DNA to damage bacterial cell walls and inhibit bacterial movement (Claudya et al., 2023). Furthermore, the antibacterial activity of all hydrogel samples will also be confirmed through total plate number testing to obtain more quantitative results. (Waresindo et al., 2021; Luthfianti et al., 2022).

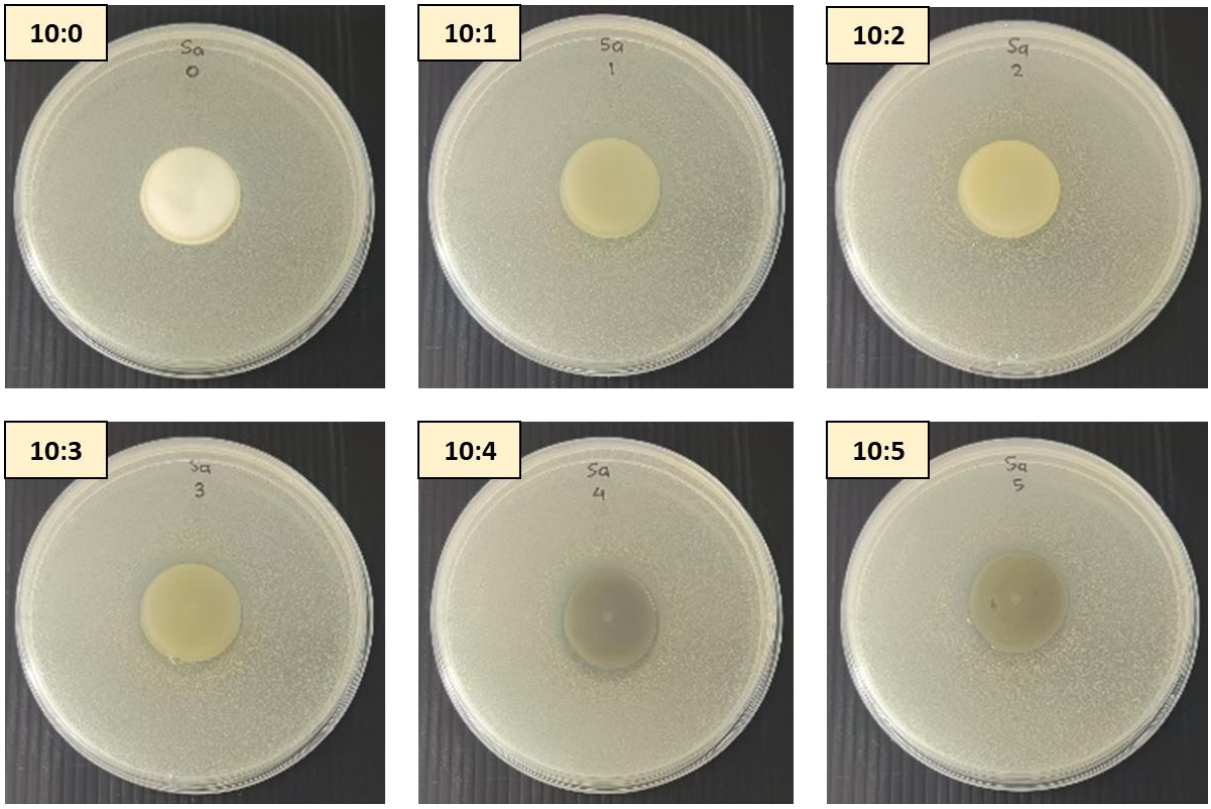

Figure 6 Image of inhibition zone against *Staphylococcus aureus* for each hydrogel sample.

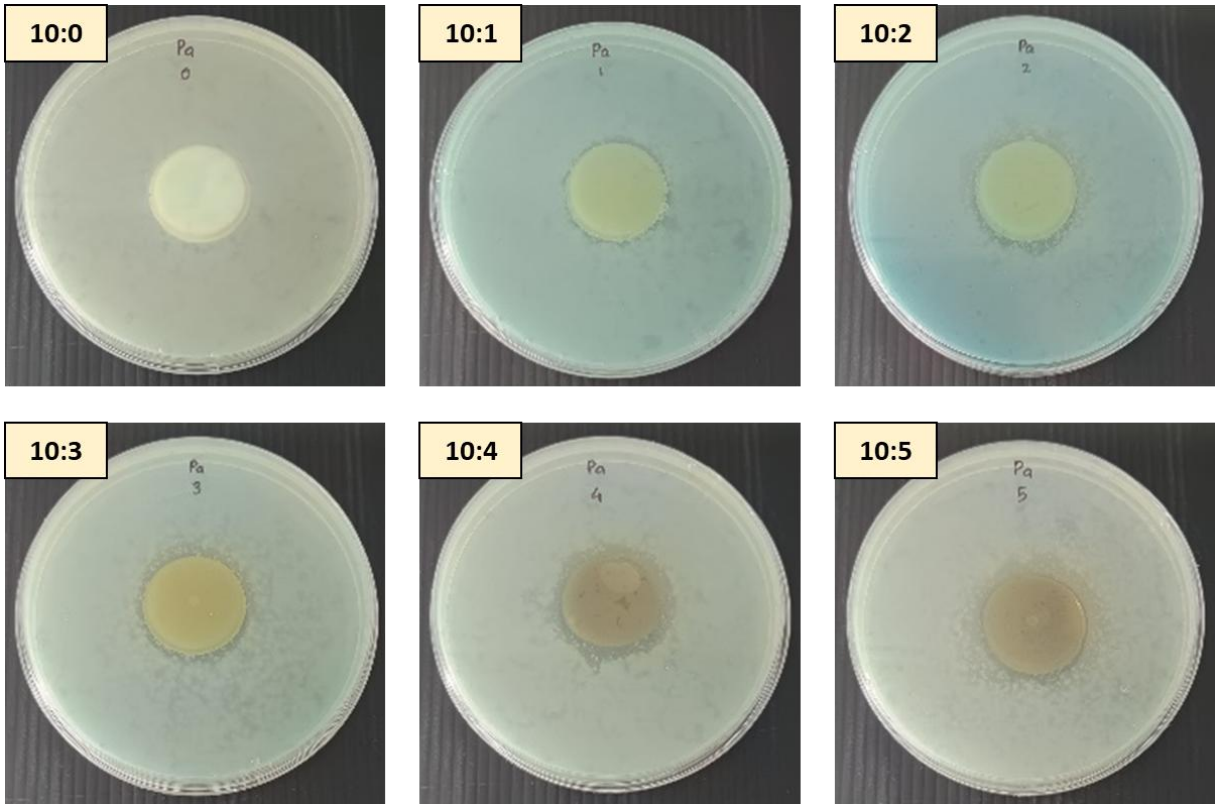

Figure 7 Image of inhibition zone against *Pseudomonas aeruginosa* for each hydrogel sample.

Table 2 Diameter of inhibition zone of the hydrogel sample.

Sample	Diameter of inhibition zone (mm)	
	S. aureus	***P. aeruginosa***
10:0	0	0
10:1	29.6	25.2
10:2	29.8	29.5
10:3	30.5	30.0
10:4	30.8	30.8
10:5	31.2	31.1

After another 24 hours of incubation, the number of bacterial colonies was counted for the control and all hydrogel samples. The image of the bacterial colonies of *Staphylococcus aureus* and *Pseudomonas aeruginosa* for each hydrogel sample is presented in Figure 8 and Figure 9. Furthermore, the antibacterial activity of all hydrogel samples is shown in Table 3. Samples 10:1 to 10:5 show excellent antibacterial activity as the extract fraction increases, consistent with the results of the increasingly larger diameter of the inhibition zone. In addition, the antibacterial activity against *Staphylococcus aureus* also appears to be higher than *Pseudomonas aeruginosa*. These results are related to differences in the cell wall structure of the two types of bacteria (Piatek et al., 2023). *Staphylococcus aureus* is known to be a gram-positive bacterium with a simple cell wall structure composed of a layer of peptidoglycan, wall teichoic acids (WTAs), and lipoteichoic acids (LTAs) (Wang et al., 2022). On the other hand, *Pseudomonas aeruginosa*, as a gram-negative bacterium, is known to have a more complex cell wall structure, which consists of huge amounts of phospholipids, lipopolysaccharides (LPS), and lipoproteins. This more complex cell wall structure then affects the decrease in cell wall permeability, making it difficult for antibacterial agents to penetrate the cell, resulting in less antibacterial activity (Alouw et al., 2022).

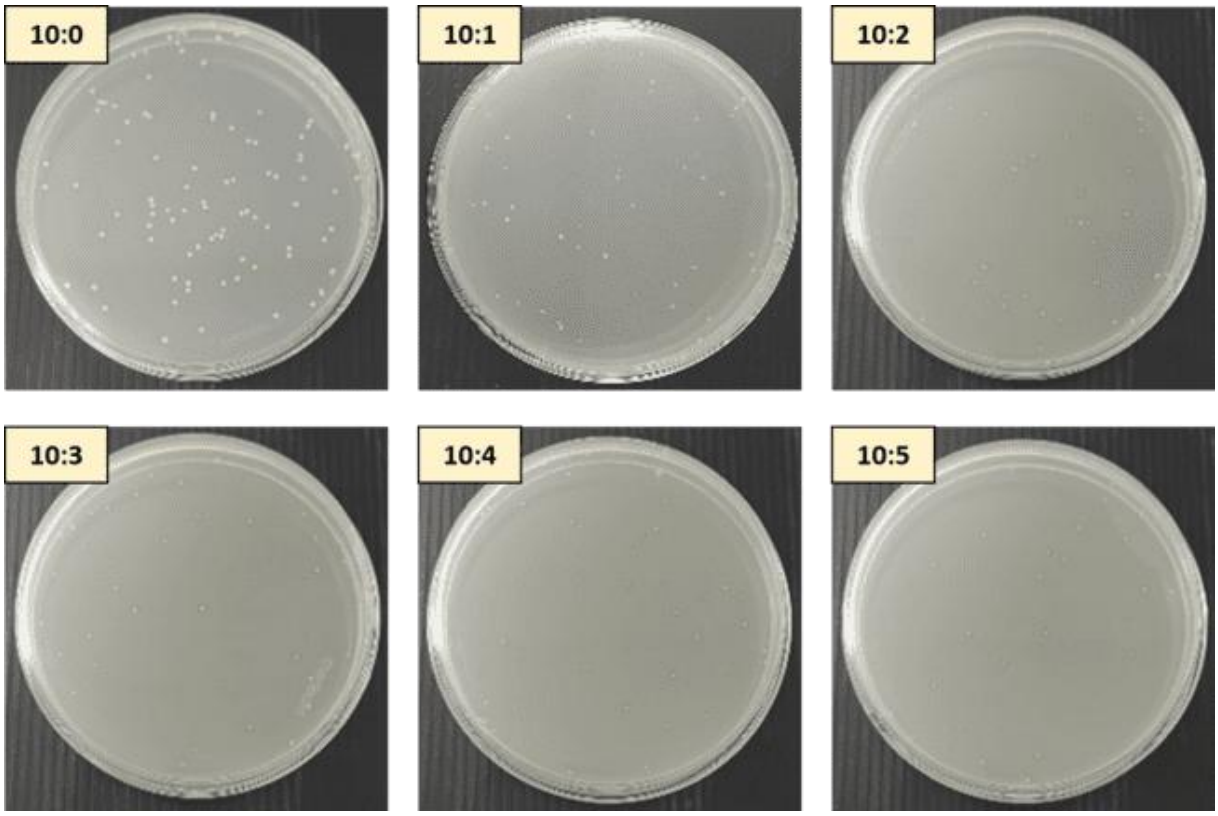

Figure 8 Image of bacterial colony of *Staphylococcus aureus*.

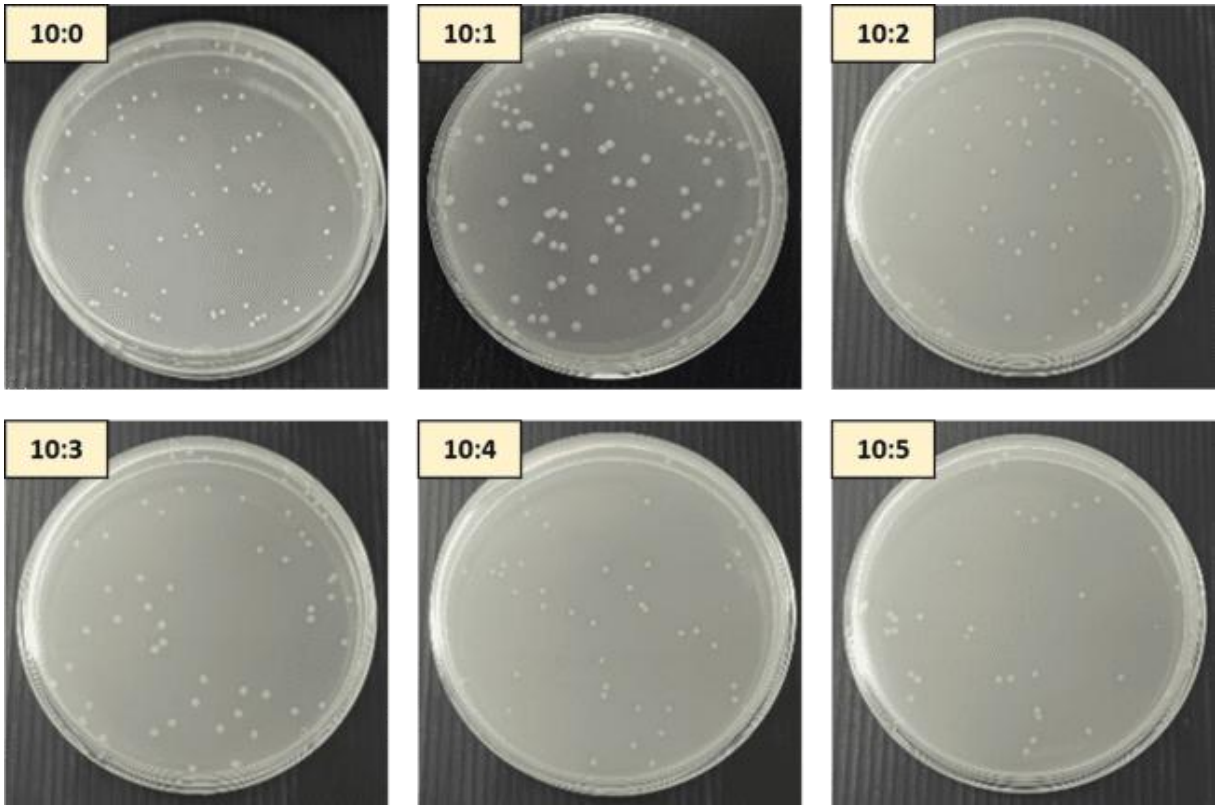

Figure 9 Image of bacterial colony of *Pseudomonas aeruginosa*.

Table 3 Antibacterial activity of hydrogel samples.

Sample	Log_{10} of bacterial colony (cfu/mL)		Antibacterial activity of hydrogels (%.gram^{-1})	
	S. aureus	***P. aeruginosa***	***S. aureus***	***P. aeruginosa***
10:0	7.80 ± 0.10	7.84 ± 0.01	0.11 ± 0.07	0.70 ± 0.06
10:1	7.65 ± 0.01	7.81 ± 0.03	1.37 ± 0.01	1.05 ± 0.23
10:2	7.58 ± 0.02	7.81 ± 0.02	2.20 ± 0.01	1.25 ± 0.18
10:3	7.53 ± 0.02	7.75 ± 0.03	2.54 ± 0.02	1.64 ± 0.23
10:4	7.45 ± 0.04	7.64 ± 0.03	4.51 ± 0.05	2.96 ± 0.27
10:5	7.38 ± 0.00	7.54 ± 0.05	4.58 ± 0.00	3.92 ± 0.52
Control	7.82 ± 0.01	7.94 ± 0.03	-	-

4. CONCLUSION

We have successfully synthesized various PVA/MCLE composite hydrogel combinations using the freeze-thaw method. The conductivity and pH of the precursor solution showed a trend of increasing values when the fraction of the extract solution increased. On the other hand, the viscosity of the precursor solution showed a decreasing value with an increasing fraction of the extract solution. The resulting hydrogel shows a morphology with increased pore size, which becomes larger when the extract fraction in the hydrogel increases. As proven by the FTIR spectrum, PVA and extracts have been successfully encapsulated in the composite hydrogels. The swelling degree of the composite hydrogel tends to increase with increasing extract fraction for samples 10:1 to 10:3. However, it tends to decrease for samples 10:4 and 10:5. On the other hand, the results of the gel fraction test prove that increasing the extract fraction in the composite hydrogel results in a decrease in the gel fraction. The antibacterial activity test also confirmed that the antibacterial activity in the extract remained visible after being encapsulated in the hydrogel. Thus, the resulting composite hydrogel has advantages in water absorption capacity and antibacterial activity, so it has promising potential for application in the biomedical field. Furthermore, this research can also be developed to determine the ability of extracts released from hydrogels and the direct application through in-vivo testing.

ACKNOWLEDGMENT

This research was financially supported by the “Direktorat Riset, Teknologi, dan Pengabdian kepada Masyarakat, Direktorat Jenderal Pendidikan Tinggi, Riset, dan Teknologi, Kementerian Pendidikan, Kebudayaan, Riset, dan Teknologi Republik Indonesia”, under the “Program Penelitian Dosen Pemula” Grant in the fiscal years of 2024.

REFERENCE

Akhtar, M. F., Hanif, M., & Ranjha, N. M. (2016). Methods of synthesis of hydrogels. *Saudi Pharmaceutical Journal*, *24*(5), 554–559. https://doi.org/10.1016/j.jsps.2015.03.022

Alouw, G., Fatimawali, F., & Lebang, J. S. (2022). Uji Aktivitas Antibakteri Ekstrak Etanol Daun Kersen (*Muntingia Calabura* L.) terhadap Bakteri *Staphylococcus Aureus* dan *Pseudomonas Aeruginosa* dengan Metode Difusi Sumuran. *Jurnal Farmasi Medica/Pharmacy Medical Journal (PMJ)*, *5*(1), 36. https://doi.org/10.35799/pmj.v5i1.41430

Anggraini, S. A., Yuniningsih, S., & Sota, M. M. (2017). Pengaruh pH terhadap Kualitas Produk Etanol dari Molasses Melalui Proses Fermentasi. *Jurnal Reka Buana*, *2*(2), 99–105. https://doi.org/10.33366/rekabuana.v2i2.725

Bashir, S., Hina, M., Iqbal, J., Rajpar, A. H., Mujtaba, M. A., Alghamdi, N. A., Wageh, S., Ramesh, K., & Ramesh, S. (2020). Fundamental Concepts of Hydrogels: Synthesis, Properties, and Their Applications. *Polymers*, *12*, 1–60. https://doi.org/https://dx.doi.org/10.3390/polym12112702

Bercea, M. (2024). Recent Advances in Poly(vinyl alcohol)-Based Hydrogels. *Polymers*, *16*(14). https://doi.org/10.3390/polym16142021

Bustamante-Torres, M., Romero-Fierro, D., Arcentales-Vera, B., Palomino, K., Magaña, H., & Bucio, E. (2021). Hydrogels classification according to the physical or chemical interactions and as stimuli-sensitive materials. *Gels*, *7*(4), 1–25. https://doi.org/10.3390/gels7040182

Caló, E., & Khutoryanskiy, V. V. (2015). Biomedical applications of hydrogels: A review of patents and commercial products. *European Polymer Journal*, *65*, 252–267. https://doi.org/10.1016/j.eurpolymj.2014.11.024

Chen, Y., Li, J., Lu, J., Ding, M., & Chen, Y. (2022). Synthesis and properties of Poly(vinyl alcohol) hydrogels with high strength and toughness. *Polymer Testing*, *108*. https://doi.org/10.1016/j.polymertesting.2022.107516

Claudya, C., Meutia, R., & Lubis, Y. E. P. (2023). Aktivitas Gel Ekstrak Daun Mengkudu (Morinda citrifolia) Terhadap Pertumbuhan Bakteri Penyebab Jerawat Staphylococcus epidermidis. *Journal of Pharmaceutical and Sciences*, *6*(4), 1645–1653. https://doi.org/10.36490/journal-jps.com.v6i4.276

Edikresnha, D., Suciati, T., Suprijadi, & Khairurrijal, K. (2021). Freeze-thawed hydrogel loaded by Piper crocatum extract with in-vitro antibacterial and release tests. *Journal of Materials Research and Technology*, *15*, 17–36. https://doi.org/https://doi.org/10.1016/j.jmrt.2021.07.151

Edikresnha, D., Suciati, T., Khairurrijal, K., & Munir, M. M. (2019). Polyvinylpyrrolidone/cellulose acetate electrospun composite nanofibres loaded by glycerine and garlic extract with in vitro antibacterial activity and release behaviour test. *RSC Advances*, *9*, 26351–26363. https://doi.org/10.1039/c9ra04072b

Erina, E., Rinidar, R., Armansyah, T., Erwin, E., Rusli, R., & Elsavira, R. (2019). Inhibitory Test of Ethanol Extract of Noni Leaf (*Morinda Citrifolia* L.) on *Staphylococcus aureus* Growth. *JIMVET*, *3*(3), 161–169. https://doi.org/10.21157/jimvet.v3i3.11377

Halimah, H., Suci, D. M., & Wijayanti, I. (2019). Study of the Potential Use of Noni Leaves (*Morinda citrifolia* L.) as an Antibacterial Agent for *Escherichia coli* and *Salmonella typhimurium*. *Jurnal Ilmu Pertanian Indonesia*, *24*, 58–64. https://doi.org/10.18343/jipi.24.1.58

Halligan, E., Tie, B. S. H., Colbert, D. M., Alsaadi, M., Zhuo, S., Keane, G., & Geever, L. M. (2023). Synthesis and Characterisation of Hydrogels Based on Poly (N-Vinylcaprolactam) with Diethylene Glycol Diacrylate. *Gels*, *9*(6). https://doi.org/10.3390/gels9060439

Hong, F., Qiu, P., Wang, Y., Ren, P., Liu, J., Zhao, J., & Gou, D. (2024). Chitosan-based hydrogels: From preparation to applications, a review. *Food Chemistry: X*, *21*(8326), 101095. https://doi.org/10.1016/j.fochx.2023.101095

Hong, H., Liao, H., Chen, S., & Zhang, H. (2014). Facile method to prepare self-healable PVA hydrogels with high water stability. *Materials Letters*, *122*, 227–229. https://doi.org/10.1016/j.matlet.2014.02.036

Hooi, M. T., Phang, S. W., Yow, H. Y., David, E., Kim, N. X., & Choo, H. L. (2021). FTIR spectroscopy characterization and critical comparison of poly(vinyl)alcohol and natural hydroxyapatite derived from fish bone composite for bone-scaffold. *Journal of Physics: Conference Series*, *2120*(1). https://doi.org/10.1088/1742-6596/2120/1/012004

Irwan, F., Afdal, A., & Arlindia, I. (2016). Kajian Hubungan Konduktivitas Listrik dengan Konsentrasi Padatan Terlarut pada Air Permukaan. *Prosiding Seminar Nasional Fisika*, *V*, 7–10. https://doi.org/10.21009/0305020102

Jayanudin, Lestari, R. S. D., Barleany, D. R., Pitaloka, A. B., Yulvianti, M., Lumbantobing, P. I., & Prasetyo, Z. E. (2024). Synthesis of polyvinyl alcohol-based polymer hydrogel as water holding in sandy soil using gamma radiation technique and its application for urea loading. *Case Studies in Chemical and Environmental Engineering*, *9*(January), 100634. https://doi.org/10.1016/j.cscee.2024.100634

Kamoun, E. A., Chen, X., Mohy, M. S., & Kenawy, E. S. (2015). Crosslinked poly(vinyl alcohol) hydrogels for wound dressing applications: A review of remarkably blended polymers. *Arabian Journal of Chemistry*, *8*, 1–14. https://doi.org/https://dx.doi.org/10.1016/j.arabjc.2014.07.005

Lazidou, D., Teknetzi, I., Karapanagiotis, I., Ritzoulis, C., & Panayiotou, C. (2019). Poly(vinyl alcohol)-borax

films as cleaning agents for icons. *Archaeological and Anthropological Sciences*, *11*, 6259–6271. https://doi.org/https://doi.org/10.1007/s12520-019-00917-1

Liang, X., Zhong, H.-J., & Ding, H. (2024). Polyvinyl Alcohol (PVA)-Based Hydrogels: Recent Progress in Fabrication, Properties, and Multifunctional Applications. *Polymers*, *16*, 2755. https://doi.org/10.3390/polym16192755

Luthfianti, H. R., Waresindo, W. X., Edikresnha, D., Chahyadi, A., Suciati, T., Noor, F. A., & Khairurrijal, K. (2022). Physicochemical Characteristics and Antibacterial Activities of Freeze-Thawed Polyvinyl Alcohol/Andrographolide Hydrogels. *ACS Omega*. https://doi.org/10.1021/acsomega.2c05110

Maeso, L., Antezana, P. E., Hvozda Arana, A. G., Evelson, P. A., Orive, G., & Desimone, M. F. (2024). Progress in the Use of Hydrogels for Antioxidant Delivery in Skin Wounds. *Pharmaceutics*, *16*(4), 1–27. https://doi.org/10.3390/pharmaceutics16040524

Maulidina, R. F., Pujiani, D., & Haryanto, H. (2022). The Effect of the Addition of Polyvinyl Alcohol (PVA) Concentrations on the Characteristics of the Carboxymethyl Cellulose (CMC)-Poly (Acrylic Acid) Hydrogel Superabsorbent as a Planting Medium. *CHEMICA: Jurnal Teknik Kimia*, *9*(2), 60. https://doi.org/10.26555/chemica.v9i2.24428

Mohammad, Z., Junaidin, J., & Yulyianti, R. (2023). Potensi Krim Ekstrak Etanol Daun Mengkudu (*Morinda Citrifolia* L .) terhadap *Staphylococcus aureus*. *Journal of Pharmacopolium*, *6*(1), 1–12. https://doi.org/10.36465/jop.v6i1.1080

Nayak, B. S., Sandiford, S., & Maxwell, A. (2009). Evaluation of the wound-healing activity of ethanolic extract of Morinda citrifolia L. leaf. *Evidence-Based Complementary and Alternative Medicine*, *6*(3), 351–356. https://doi.org/10.1093/ecam/nem127

Parmadi, A., Rejeki, S., & Hastuti, S. (2019). Effectiveness and Evaluation Test of All Cream of Ethanol Extract of Noni Leaf (*Morinda citrifolia* L) as Wound Healing Medicine. *Indonesian Journal On Medical Science*, *6*(1), 13–19.

Pertiwi, Y. U. P. P., Prajitno, A., & Fadjar, M. (2019). Analysis of Metabolit And Antibacterial Control of Mengkudu Leaf Extract (*Morinda citrifolia*) on the Bacteria of *Aeromonas hydrophila*. *Research Journal of Life Science*, *6*(3), 172–183. https://doi.org/10.21776/ub.rjls.2019.006.03.3

Piatek, M., O'Beirne, C., Beato, Z., Tacke, M., & Kavanagh, K. (2023). Pseudomonas aeruginosa and Staphylococcus aureus Display Differential Proteomic Responses to the Silver(I) Compound, SBC3. *Antibiotics*, *12*(2), 1–16. https://doi.org/10.3390/antibiotics12020348

Preda, M. D., Popa, M. L., Neacșu, I. A., Grumezescu, A. M., & Ginghină, O. (2023). Antimicrobial Clothing Based on Electrospun Fibers with ZnO Nanoparticles. *International Journal of Molecular Sciences*, *24*(2). https://doi.org/10.3390/ijms24021629

Puspitasari, T., Raja, K. M. L., Pangerteni, D. S., Patriati, A., & Putra, E. G. R. (2012). Structural Organization of Poly(vinyl alcohol) Hydrogels Obtained by Freezing/Thawing and Gamma-Irradiation Processes: A Small-Angle Neutron Scattering (SANS) Study. *Procedia Chemistry*, *4*, 186–193. https://doi.org/10.1016/j.proche.2012.06.026

Qiao, L., Liang, Y., Chen, J., Huang, Y., Alsareii, S. A., Manaa, A., Harraz, F. A., & Guo, B. (2023). Antibacterial conductive self-healing hydrogel wound dressing with dual dynamic bonds promotes infected wound healing. *Bioactive Materials*, *30*, 129–141. https://doi.org/10.1016/j.bioactmat.2023.07.015

Ramadhani, F., Miratsi, L., Humaeroh, Z., & Afriani, F. (2021). Sintesis dan Karakterisasi Hidrogel PVA/Alginat Mengandung Ekstrak Lada sebagai Pembalut Luka Antibakteri. *Newton-Maxwell Journal of Physics*, *2*(2), 54–59. https://doi.org/10.33369/nmj.v2i2.17752

Sabirin, I. P. R., Maskoen, A. M., & Hernowo, B. S. (2013). Peran Ekstrak Etanol Topikal Daun Mengkudu (*Morinda citrifolia* L.) pada Penyembuhan Luka Ditinjau dari Imunoekspresi CD34 dan Kolagen pada Tikus Galur Wistar. *Majalah Kedokteran Bandung*, *45*(4), 226–233. https://doi.org/10.15395/mkb.v45n4.169

Saputro, M. R., Windhu Wardhana, Y., & Wathoni, N. (2021). Stabilitas Hidrogel dalam Penghantaran Obat. *Majalah Farmasetika*, *6*(5), 421. https://doi.org/10.24198/mfarmasetika.v6i5.35705

Sarkar, B., Bhattacharya, P., Chen, C., & Maity, J. P. (2022). A comprehensive characterization and therapeutic

properties in ripened Noni fruits (*Morinda citrifolia* L.). *International Journal of Experimentall Research and Review*, *29*, 10–32. https://doi.org/10.52756/ijerr.2022.v29.002

Savić Gajić, I. M., Savić, I. M., & Svirčev, Z. (2023). Preparation and Characterization of Alginate Hydrogels with High Water-Retaining Capacity. *Polymers*, *15*(12). https://doi.org/10.3390/polym15122592

Stabik, J., Dybowska, A., & Szczepanik, M. (2009). Viscosity measurements of epoxy resin filled with ferrite powders. *Archives of Materials Science and Engineering*, *38*, 34–40.

T, S. M., AbdulWahhab, N. A., & Al-Araji, A. H. (2023). Study the Optical Properties of Polyvinyl Alcohol Thick Film Irradiated with Violet Laser. *Journal of University of Babylon for Pure and Applied Sciences*, *31*(3), 137–146. https://doi.org/10.29196/jubpas.v31i3.4834

Wang, M., Buist, G., & Dijl, J. M. Van. (2022). *Staphylococcus aureus* cell wall maintenance – the multifaceted roles of peptidoglycan hydrolases in bacterial growth, fitness, and virulence. *FEMS microbiology reviews*, 1–19. https://doi.org/10.1093/femsre/fuac025

Wang, R., Cheng, C., Wang, H., & Wang, D. (2024). Swollen hydrogel nanotechnology: Advanced applications of the rudimentary swelling properties of hydrogels. *ChemPhysMater*, *3*, 357–375. https://doi.org/10.1016/j.chphma.2024.07.006

Wang, Z., Ye, Q., Yu, S., & Akhavan, B. (2023). Poly Ethylene Glycol (PEG)-Based Hydrogels for Drug Delivery in Cancer Therapy: A Comprehensive Review. *Advanced Healthcare Materials*, *12*(18), 1–21. https://doi.org/10.1002/adhm.202300105

Waresindo, W. X., Luthfianti, H. R., Edikresnha, D., Suciati, T., Noor, F. A., & Khairurrijal, K. (2021). A freeze–thaw PVA hydrogel loaded with guava leaf extract: physical and antibacterial properties. *RSC Advances*, *11*, 30156–30171. https://doi.org/10.1039/D1RA04092H

Zhang, C., Qi, Y., & Zhang, Z. (2022). Swelling Behaviour of Polystyrene Microsphere Enhanced PEG-Based Hydrogels in Seawater and Evolution Mechanism of Their Three-Dimensional Network Microstructure. *Materials*, *15*(14). https://doi.org/10.3390/ma15144959

Zhao, L., Zhou, Y., Zhang, J., Liang, H., Chen, X., & Tan, H. (2023). Natural Polymer-Based Hydrogels: From Polymer to Biomedical Applications. *Pharmaceutics*, *15*(10). https://doi.org/10.3390/pharmaceutics15102514

Zidan, H. M., Abdelrazek, E. M., Abdelghany, A. M., & Tarabiah, A. E. (2019). Characterization and some physical studies of PVA/PVP filled with MWCNTs. *Journal of Materials Research and Technology*, *8*(1), 904–913. https://doi.org/10.1016/j.jmrt.2018.04.023